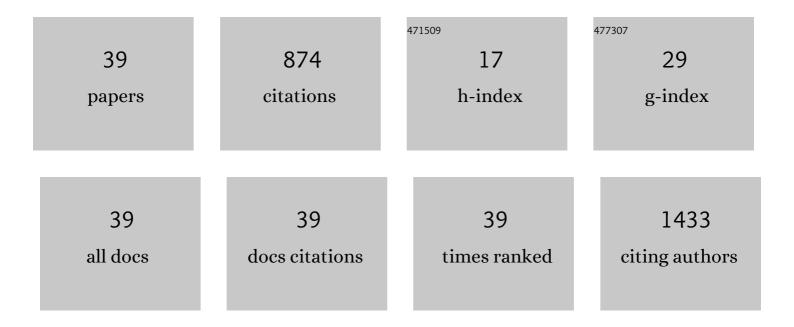
Eun-Kee Jeong

List of Publications by Year in descending order

Source: https://exaly.com/author-pdf/6023951/publications.pdf Version: 2024-02-01



#	Article	IF	CITATIONS
1	High-resolution DTI with 2D interleaved multislice reduced FOV single-shot diffusion-weighted EPI (2D) Tj ETQq1	1 9.78431	.4 ₁₈₈ T/Ove
2	Symmetryâ€Guided Design and Fluorous Synthesis of a Stable and Rapidly Excreted Imaging Tracer for ¹⁹ Fâ€MRI. Angewandte Chemie - International Edition, 2009, 48, 4755-4758.	13.8	101
3	High-resolution diffusion-weighted 3D MRI, using diffusion-weighted driven-equilibrium (DW-DE) and multishot segmented 3D-SSFP without navigator echoes. Magnetic Resonance in Medicine, 2003, 50, 821-829.	3.0	58
4	Decreased brain <scp>PME</scp> / <scp>PDE</scp> ratio in bipolar disorder: a preliminary ³¹ P magnetic resonance spectroscopy study. Bipolar Disorders, 2015, 17, 743-752.	1.9	52
5	Noninvasive Visualization of Pharmacokinetics, Biodistribution and Tumor Targeting of Poly[N-(2-hydroxypropyl)methacrylamide] in Mice Using Contrast Enhanced MRI. Pharmaceutical Research, 2007, 24, 1208-1216.	3.5	50
6	High-resolution DTI of a localized volume using 3Dsingle-shot diffusion-weightedSTimulatedecho-planarimaging (3D ss-DWSTEPI). Magnetic Resonance in Medicine, 2006, 56, 1173-1181.	3.0	42
7	<i>InÂvivo</i> evidence of an age-related increase in ATP cost of contraction in the plantar flexor muscles. Clinical Science, 2014, 126, 581-592.	4.3	34
8	Examination of penetration routes and distribution of ionic permeants during and after transscleral iontophoresis with magnetic resonance imaging. International Journal of Pharmaceutics, 2007, 335, 46-53.	5.2	33
9	Wideband late gadolinium enhanced magnetic resonance imaging for imaging myocardial scar without image artefacts induced by implantable cardioverter-defibrillator: a feasibility study at 3 T. Europace, 2015, 17, 483-488.	1.7	31
10	Skeletal muscle work efficiency with age: the role of non-contractile processes. Clinical Science, 2015, 128, 213-223.	4.3	26
11	Wideband arrhythmiaâ€Insensitiveâ€rapid (AIR) pulse sequence for cardiac T1 mapping without image artifacts induced by an implantableâ€cardioverterâ€defibrillator. Magnetic Resonance in Medicine, 2015, 74, 336-345.	3.0	23
12	Accuracy of Diffusion Tensor Imaging for Diagnosing Cervical Spondylotic Myelopathy in Patients Showing Spinal Cord Compression. Korean Journal of Radiology, 2015, 16, 1303.	3.4	23
13	Accuracy and precision of quantitative ³¹ P-MRS measurements of human skeletal muscle mitochondrial function. American Journal of Physiology - Endocrinology and Metabolism, 2016, 311, E358-E366.	3.5	23
14	Measurement of creatine kinase reaction rate in human brain using magnetization transfer imageâ€selected <i>in vivo</i> spectroscopy (MTâ€ISIS) and a volume ³¹ P/ ¹ H radiofrequency coil in a clinical 3â€T MRI system. NMR in Biomedicine, 2011, 24, 765-770.	2.8	22
15	Reduction of flow-related signal loss in flow-compensated 3D TOF MR angiography, using variable echo time (3D TOF-VTE). Magnetic Resonance in Medicine, 2002, 48, 667-676.	3.0	21
16	Effect of altitude on brain intracellular pH and inorganic phosphate levels. Psychiatry Research - Neuroimaging, 2014, 222, 149-156.	1.8	21
17	Maximal strength training increases muscle force generating capacity and the anaerobic ATP synthesis flux without altering the cost of contraction in elderly. Experimental Gerontology, 2018, 111, 154-161.	2.8	20
18	Evidence of Preserved Oxidative Capacity and Oxygen Delivery in the Plantar Flexor Muscles With Age. Journals of Gerontology - Series A Biological Sciences and Medical Sciences, 2015, 70, 1067-1076.	3.6	18

Eun-Kee Jeong

#	Article	IF	CITATIONS
19	Anterior cingulate cortex choline levels in female adolescents with unipolar versus bipolar depression: A potential new tool for diagnosis. Journal of Affective Disorders, 2014, 167, 25-29.	4.1	17
20	Changes of Neurotransmitters in Youth with Internet and Smartphone Addiction: A Comparison with Healthy Controls and Changes after Cognitive Behavioral Therapy. American Journal of Neuroradiology, 2020, 41, 1293-1301.	2.4	17
21	Ocular pharmacokinetic study of a corticosteroid by 19F MR. Experimental Eye Research, 2010, 91, 347-352.	2.6	16
22	Impaired Muscle Efficiency but Preserved Peripheral Hemodynamics and Mitochondrial Function With Advancing Age: Evidence From Exercise in the Young, Old, and Oldest-Old. Journals of Gerontology - Series A Biological Sciences and Medical Sciences, 2018, 73, 1303-1312.	3.6	16
23	Impact of age on exercise-induced ATP supply during supramaximal plantar flexion in humans. American Journal of Physiology - Regulatory Integrative and Comparative Physiology, 2015, 309, R378-R388.	1.8	13
24	Synchronous radial ¹ H and ²³ Na dualâ€nuclear <scp>MRI</scp> on a clinical <scp>MRI</scp> system, equipped with a broadband transmit channel. Concepts in Magnetic Resonance Part B, 2016, 46B, 191-201.	0.7	12
25	Improvement of accuracy of diffusion MRI using realâ€ŧime selfâ€gated data acquisition. NMR in Biomedicine, 2009, 22, 545-550.	2.8	10
26	Skeletal Muscle Mitochondrial Adaptations to Maximal Strength Training in Older Adults. Journals of Gerontology - Series A Biological Sciences and Medical Sciences, 2020, 75, 2269-2277.	3.6	10
27	Two-dimensional single-shot diffusion-weighted stimulated EPI with reduced FOV for ultrahigh-b radial diffusion-weighted imaging of spinal cord. Magnetic Resonance in Medicine, 2017, 77, 2167-2173.	3.0	9
28	Oxygen delivery and the restoration of the muscle energetic balance following exercise: implications for delayed muscle recovery in patients with COPD. American Journal of Physiology - Endocrinology and Metabolism, 2017, 313, E94-E104.	3.5	9
29	Evidence of a metabolic reserve in the skeletal muscle of elderly people. Aging, 2016, 9, 52-67.	3.1	9
30	Diffusion tensor imaging focusing on lower cervical spinal cord using 2D reduced FOV interleaved multislice single-shot diffusion-weighted echo-planar imaging: comparison with conventional single-shot diffusion-weighted echo-planar imaging. Magnetic Resonance Imaging, 2015, 33, 401-406.	1.8	8
31	Characterization of spinal cord white matter by suppressing signal from hindered space. A Monte Carlo simulation and an ex vivo ultrahigh-b diffusion-weighted imaging study. Journal of Magnetic Resonance, 2016, 272, 53-59.	2.1	7
32	Eightâ€channel decoupled array for cervical spinal cord imaging at 3T: sixâ€channel posterior and twoâ€channel anterior array coil. Concepts in Magnetic Resonance Part B, 2016, 46B, 90-99.	0.7	5
33	Study of kinetics of 19F-MRI using a fluorinated imaging agent (19FIT) on a 3T clinical MRI system. Magnetic Resonance Materials in Physics, Biology, and Medicine, 2019, 32, 97-103.	2.0	4
34	Evaluation of CLT1-(Gd-DTPA) for Cancer MR Molecular Imaging in a Mouse Breast Cancer Model. Bopuxue Zazhi, 2011, 2, 325-330.	1.0	4
35	Ultraâ€highâ€b radial diffusionâ€weighted imaging (UHbâ€rDWI) of human cervical spinal cord. Journal of Magnetic Resonance Imaging, 2019, 49, 204-211.	3.4	3
36	Diffusion MRI using two-dimensional single-shot radial imaging (2D ss-rDWI) with variable flip angle and random view ordering. Magnetic Resonance Imaging, 2019, 61, 273-284.	1.8	2

Eun-Kee Jeong

#	Article	IF	CITATIONS
37	Ultrahighâ€b diffusionâ€weighted imaging for quantitative evaluation of myelination in shiverer mouse spinal cord. Magnetic Resonance in Medicine, 2022, 87, 179-192.	3.0	2
38	Continuous prospectively navigated multiâ€echo GRE for improved BOLD imaging of the kidneys. NMR in Biomedicine, 2019, 32, e4078.	2.8	1
39	Shortâ€ŧerm training alters the control of mitochondrial respiration rate before maximal oxidative ATP synthesis. FASEB Journal, 2013, 27, 1202.1.	0.5	0